Robust Control of a 2D Rehabilitation Robot Using Admittance and RBF Neural Network

I.V. Merkuryev [1], T. B. Duishenaliev [1], Guijun Wu [2,3,*], and Z. Z. Dotalieva [2]

[1] Department of Robotics, Mechatronics, Dynamics and Strength of Machines, National Research University Moscow Power Engineering Institute, Moscow, Russia
[2] Department of Mechanics and Industrial Engineering, Kyrgyz-German Technical Institute, Kyrgyz State Technical University named after I. Razzakov, Bishkek, Kyrgyzstan
[3] Department of Mechanical Engineering, Anyang Institute of Technology, Anyang, China
Email: merkuryeviv@mpei.ru (I.V.M.); duyshenaliyevt@mpei.ru (T.B.D.); wuguijun957@gmail.com (G.W.); zh.dotalieva@kstu.kg (Z.Z.D.)
*Corresponding author

Abstract—**Control of Two-Dimensional (2D) rehabilitation robots is inherently challenged by nonlinearities, time-varying uncertainties, and modeling inaccuracies, which can significantly undermine compliance and tracking performance during human-robot interactions. To address these challenges, this paper presents a robust hybrid control strategy that integrates admittance control, adaptive Radial Basis Function (RBF) neural network compensation, and sliding mode control. Within this framework, admittance control is utilized to generate a compliant reference velocity based on the measured interaction force. The adaptive RBF neural network functions to estimate unmodeled nonlinear dynamics in real-time, operating without the need for prior system knowledge. Additionally, sliding mode control is employed to mitigate estimation errors and enhance system robustness. Stability analysis, grounded in Lyapunov theory, is performed to confirm the boundedness of the overall closed-loop system. Simulation and experimental results substantiate the efficacy of the proposed strategy in augmenting tracking accuracy and improving disturbance rejection. Preliminary simulation findings reveal that, compared to conventional admittance and sliding mode controllers that lack RBF integration, the proposed method achieves a reduction in root mean square tracking error by up to 95.0% (from 0.5658 m/s to 0.0285 m/s), and a decrease in maximum velocity tracking error by 51.7% (from 0.8552 m/s to 0.4132 m/s). Moreover, the system recovers to the desired state within 0.08 seconds, while the baseline method fails to stabilize within a 5-second simulation interval. These results highlight the superior disturbance rejection and rapid recovery capabilities inherent in the proposed RBF-enhanced control strategy. Collectively, these findings suggest that the proposed approach holds significant promise for ensuring reliable and precise rehabilitation motions within nonlinear and uncertain environments.**

Keywords—**admittance control, Radial Basis Function (RBF) neural network, sliding mode control, adaptive control, rehabilitation robot**

I. Introduction

The application of rehabilitation robots in the field of medical rehabilitation is becoming increasingly popular, especially for patients who have movement disorders due to accidents or diseases. This technology shows good prospects [1, 2]. These systems can provide repetitive exercise training, help patients improve motor coordination, and significantly reduce the workload of therapists in clinical environments. Therefore, rehabilitation robots have attracted widespread attention from researchers and clinical practitioners [3]. However, a major challenge in actual training is how to achieve safe, smooth, and high-precision human-computer interaction in the presence of individual patient differences, unmodeled system dynamics, and external interference.

The rapid advancements in extremity rehabilitation have driven the development of multiple lower-limb exoskeleton prototypes, including Ekso (US), HAL (Japan), ReWalk (Israel), and HIT-LEX (China), which have demonstrated preliminary clinical efficacy [4, 5]. However, critical limitations persist in their control architectures that necessitate further refinement. While conventional Sliding Mode Control (SMC) exhibits robust disturbance rejection in exoskeleton implementations, its characteristic high-frequency control chattering induces accelerated mechanical degradation and potential patient discomfort [6]. Furthermore, model-dependent control frameworks frequently prove inadequate when confronted with parametric uncertainties and exogenous perturbations, significantly constraining their clinical applicability [7].

The efficacy of rehabilitation robotics is fundamentally contingent upon control strategy optimization, which governs three critical performance metrics: therapeutic outcome quality, user comfort level, and operational safety assurance. Existing approaches generally suffer from excessive dependence on precise dynamic modeling,

Manuscript received April 7, 2025; revised April 28, 2025; accepted June 12, 2025; published September 19, 2025.

inadequate disturbance rejection capability, and high-frequency oscillations in control signals, which have severely impeded clinical translation [8]. Therefore, there is an urgent need to develop a control strategy capable of accurately compensating for unknown disturbances in real time while improving system tracking performance and robustness [9]. Successful implementation of such strategies could potentially elevate functional recovery rates, reduce patient-reported discomfort indices, and accelerate the clinical translation of rehabilitation robot technologies [10].

In recent years, adaptive control strategies have been widely investigated to address modeling errors and unknown disturbances. Among them, Radial Basis Function (RBF) neural networks have been extensively applied for real-time estimation and compensation of unmodeled dynamics and external disturbances in robotic systems, owing to their strong nonlinear approximation capability, fast online learning, and independence from precise system models. While RBF networks enhance the adaptability of control systems, their robustness remains constrained under sudden disturbances or inadequate excitation conditions. Therefore, the synergistic integration of RBF neural networks with sliding mode control to develop a composite strategy that facilitates both disturbance estimation and robust compensation emerges as a promising avenue for enhancing overall system performance.

Based on the aforementioned analysis, this paper introduces a novel control strategy that harnesses the capabilities of an RBF neural network for the estimation of external disturbances. This is subsequently followed by robust compensation of the estimated errors utilizing a sliding mode controller. To address the issue of high-frequency chattering commonly associated with sliding mode control, the introduced control law incorporates a smooth activation function, specifically the hyperbolic tangent (tanh). This modification effectively mitigates discontinuities typically encountered with traditional sign functions. Furthermore, the compensatory effect provided by the RBF network diminishes the necessity for excessively high control gains within the sliding mode controller, thereby ensuring system robustness and stability even under relatively mild activation conditions. Consequently, this enhances the overall smoothness and comfort experienced during human-robot interactions.

In light of this analysis, our research proposes a hybrid control strategy that amalgamates admittance control, adaptive RBF neural network estimation, and smooth sliding mode compensation tailored for Two-Dimensional (2D) rehabilitation robots. The primary objectives of this study are outlined as follows:

(1) To facilitate compliant interactions between the robot and the patient through the implementation of admittance control, transforming the applied human forces into the desired motion velocities. This approach significantly improves both safety and comfort throughout the rehabilitation process.
(2) To achieve real-time estimation and compensation for unknown nonlinear dynamics, leveraging an adaptive RBF neural network.
(3) To integrate RBF-based disturbance compensation with a tanh-based sliding mode control law, thereby enhancing the robustness of the system while effectively mitigating high-frequency chattering.

The main contributions of this paper are summarized as follows:

(1) A hybrid control framework is proposed, integrating admittance control, SMC, and adaptive RBF neural network compensation. This architecture enhances the robot's ability to handle external disturbances and dynamic uncertainties while maintaining compliant and safe human–robot interaction.
(2) A novel velocity-tracking control law is developed based on velocity-level error dynamics and nonlinear compensation. This formulation significantly improves tracking accuracy and robustness under varying operational conditions.
(3) The proposed method is validated through both MATLAB simulations and hardware experiments. Comparative analyses are conducted using quantitative performance metrics, including Root Mean Square Error (RMSE), maximum tracking error, and recovery time, to demonstrate the superior effectiveness of the proposed controller over traditional approaches.

The proposed integrated control framework aspires to concurrently enhance trajectory tracking accuracy, dynamic response speed, and compliance in human-robot interactions. Comprehensive simulations and experimental validations have been conducted to assess the performance and feasibility of the proposed method, showcasing its promising potential for practical applications in rehabilitation training.

II. Literature Review

In recent years, a diverse array of compensation control methodologies has been progressively implemented in rehabilitation robotics to counteract modeling inaccuracies and external disturbances [11]. For instance, Ding *et al*. [12] proposed an admittance controller that significantly mitigates interaction impacts between patients and robotic systems; however, this approach exhibits limited adaptability to nonlinear disturbances and complex dynamic characteristics [13]. SMC, known for its robustness, is widely adopted in this field, yet traditional implementations of SMC are plagued by high-frequency chattering, which hinders practical application [14].

To overcome these issues, Shi *et al*. [15] conceptualized a control strategy that amalgamates Proportional-Integral-Derivative (PID) control with RBF neural networks. This innovative approach capitalizes on the self-learning capabilities of neural networks to compensate for nonlinearities and uncertainties inherent in the system. However, it is noteworthy that neural-network-based control schemes often grapple with slow convergence rates

and susceptibility to local minima, rendering them less ideal for real-time rehabilitation applications [16]. Furthermore, Hussain pointed out that despite the robustness conferred by SMC, this method introduces increased complexity in controller design and fails to entirely mitigate the phenomenon of chattering [17].

These theoretical challenges are mirrored in practical rehabilitation devices. For instance, the Ekso exoskeleton robot, developed by Ekso Bionics (USA), supports multiple training modalities to cater to varying rehabilitation stages. Similarly, the HAL system from the University of Tsukuba (Japan) employs electromyographic sensors to discern user motion intent, facilitating intention-based active control [18]. The ReWalk exoskeleton from ReWalk Robotics (Israel) employs an array of sensors to dynamically modify motion strategies according to the user's movements. Additionally, the HIT-LEX robot from Harbin Institute of Technology (China) is distinguished by its lightweight design and enhanced compliance control capabilities [6]. Moreover, Zaway *et al*. [19] proposed a multi-objective Fractional-Order PID (FOPID) optimization strategy specifically targeted at pediatric gait rehabilitation, employing a genetic algorithm for tuning controller parameters aimed at minimizing error, energy consumption, and startup torque.

Notwithstanding the advancements represented by these studies and commercial solutions, several common challenges persist [20]. Firstly, conventional model-based control methodologies rely extensively on accurate dynamic models, displaying limited adaptability to individual variations [21]. Secondly, while SMC is heralded for its robustness, its tendency to induce severe chattering can compromise device stability and user comfort [22]. Lastly, single-strategy control methodologies often encounter difficulties in achieving a satisfactory balance between high tracking accuracy, real-time responsiveness, and necessary interaction compliance [23].

In recent studies, researchers have begun to explore hybrid frameworks that integrate RBF neural networks with SMC. Within these systems, the RBF network functions estimate external disturbances and model uncertainties in real time, while the sliding term provides robust error compensation. in an adaptive hybrid control structure. This approach reduces dependency on precise system modeling and enhances the system's disturbance rejection capability.

In addition, traditional SMC faces inherent high-frequency switching problems, such as mechanical oscillations caused by sudden control transitions. In order to improve the continuity of control signals and user experience, researchers have incorporated smooth activation functions such as hyperbolic tangent (tanh) functions into control design [24].

Overall, robust performance [25], high precision, and compatible human-robot interaction remain the top priorities in the development of rehabilitation robot control systems. The hybrid control strategy integrating admittance regulation, RBF neural networks, and sliding mode techniques has been established as a robust solution to address these interdisciplinary challenges [26]. The control method proposed in this paper builds upon this trend and further optimizes the controller structure and disturbance compensation capabilities.

III. Materials and Methods

A. Structure and Dynamic Analysis of the Rehabilitation Robot

The 2D rehabilitation robot employed in this study consists of two planar motion mechanisms arranged perpendicularly in the x and y directions. A handle is mounted on the upper x-direction mechanism to allow the patient to grip and interact with the robot. A two-dimensional force sensor (sensing forces in both x and y directions) is installed at the lower end of the handle to perceive the patient's movement intentions in real time in any direction on the plane. A display screen is used to show the handle's motion trajectory, interactive games, and other related information.

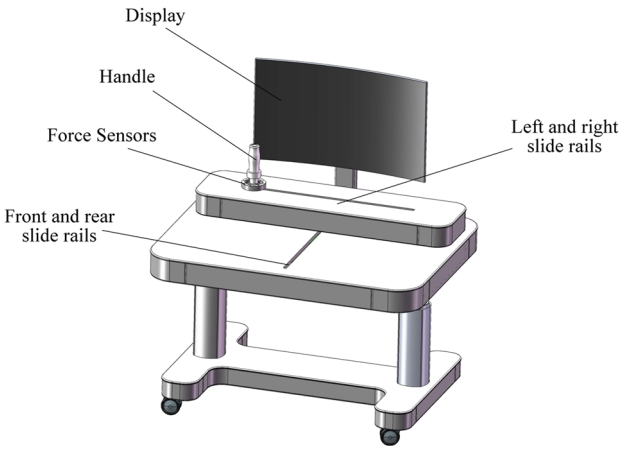

Fig. 1. 2D rehabilitation robot.

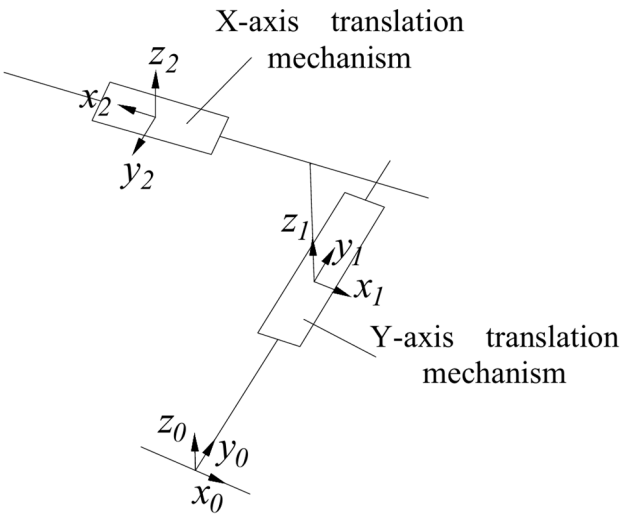

Fig. 2. Coordinate system of the rehabilitation robot.

This rehabilitation robot offers four distinct control modes: active, passive, assistive, and impedance control. Notably, the active mode is the most frequently employed

but also presents considerable implementation challenges. In this mode, the handle is designed to respond to the user's gentle guidance with a high degree of compliance, facilitating zero-force control [27, 28]. The control approach proposed in this study aims to accomplish such zero-force control effectively. The architecture of the 2D rehabilitation robot and its corresponding coordinate system are illustrated in Fig. 1.

Based on the structure of the rehabilitation robot, the coordinate system of the upper-limb rehabilitation robot is established, as shown in Fig. 2.

Utilizing this coordinate framework, the dynamic model of the 2D rehabilitation robot is established to enable motion control of the robot. The dynamic equation of the rehabilitation robot can be written in the standard form, as shown in Eq. (1):

$$M(q)\ddot{q} + C(q,\dot{q})\dot{q} + F(\dot{q}) + G(q) = F \quad (1)$$

where:
q,$\dot{q}$,$\ddot{q}$: denote the position, velocity, and acceleration of the moving joints, respectively;
F: is the driving force generated by the motors;
$M(q) \in R^{1\times1}$: represents the inertial force term caused by the acceleration of the handle mass;
$C(q,\dot{q}) \in R^{1x1}$: denotes the Coriolis and centrifugal forces;
$F(\dot{q}) \in R^{1\times1}$: represents the friction force;
$G(q) \in R^{1\times1}$: is the gravitational force term.

The rehabilitation robot investigated in this study is engineered as a two-Degree-of-Freedom (2-DOF) planar system, comprising two orthogonally positioned and independently actuated translational modules. To facilitate the analysis of dynamic interactions between the two axes, a comprehensive coupled dynamic model is established, as shown in Eq. (2):

$$\begin{bmatrix} m_x & m_{xy} \\ m_{yx} & m_y \end{bmatrix}\begin{bmatrix} \ddot{x} \\ \ddot{y} \end{bmatrix} + \begin{bmatrix} d_x & d_{xy} \\ d_{yx} & d_y \end{bmatrix}\begin{bmatrix} \dot{x} \\ \dot{y} \end{bmatrix} = \begin{bmatrix} F_x \\ F_y \end{bmatrix} \quad (2)$$

The terms m_{xy} , m_{yx} , d_{xy} , and d_{yx} represent the cross-axis inertial and damping coupling terms. Such a matrix-based formulation is commonly employed in the analysis of multivariable mechanical systems, including robotic manipulators and mechatronic platforms.

Preliminary experimental tests and structural symmetry analysis indicate that these coupling terms are relatively small, Thus, the coupled model can be approximated as dynamically decoupled, as shown in Eq. (3):

$$m_x \cdot \ddot{x} = F_x, \; m_y \cdot \ddot{y} = F_y \quad (3)$$

This simplification allows for independent controller design on each axis and significantly reduces computational complexity during real-time implementation.

Therefore, the control strategies for the two motion mechanisms can be independently evaluated by transforming them into one-dimensional motion systems. Given that the control algorithms for both axes are analogous, this paper will focus exclusively on the analysis of the x-direction motion mechanism.

In this study, the motor driving force is utilized to actuate a sliding module, which subsequently translates the handle. The transmission of force is contingent upon the mechanical structure, which may include components such as electric actuators or lead screws. For the purpose of analysis, we will focus exclusively on the driving force transmitted to the handle via the associated transmission mechanism.

The rehabilitation robot under consideration is a quintessential example of a nonlinear system, with its performance being highly sensitive to uncertainties in model parameters and external disturbances. The simplified dynamic equation of the system is described in Eq. (4):

$$M\dot{v} = F_m + F_{ex} - F_{dist} - F_{fric} - \Delta(x,v) \quad (4)$$

In the equation:
M: mass of the handle;
$\dot{v}$: acceleration of the handle;
F_m: motor output force;
F_{ex}: interaction force measured by the sensor;
F_{dist} : external disturbance force (e.g., environmental forces, sudden impacts);
F_{fric}: friction force (e.g., sliding friction, air resistance);
$\Delta(x,v)$: represents the modeling error in the system.

Based on the system dynamics and the interaction forces exerted on the handle, the desired handle velocity is generated using an admittance control approach. The motor actuates the handle via a transmission mechanism, enabling it to follow the specified velocity in a compliant manner, thereby facilitating compliant motion control.

Informed by the established dynamics, the subsequent control strategy is developed in a systematic sequence, commencing with the outer-loop admittance control, progressing to the inner-loop robust controller, and culminating in the synthesis of the complete control law.

B. Admittance Control

The outer-loop admittance controller is designed to produce a compliant desired velocity that reacts to the forces exerted by the user, which will subsequently serve as the input for the inner-loop robust controller.

The essence of admittance control lies in its capacity to convert the measured interaction force into a desired velocity, as noted in Ref. [29]. A significant advantage of this approach is its ability to achieve compliant control without necessitating an accurate dynamic model of the robotic system. Given the complexities involved in dynamic modeling of robots—where frictional effects can be challenging to quantify precisely [30] and external disturbances often manifest unpredictably—admittance control is particularly well-suited for active compliant control applications in upper limb rehabilitation training robots.

The active motion control of the upper-limb rehabilitation robot can be described by the following differential Eq. (5):

$$M_d\dot{v}_d + B_d v_d + K_d \int v_d = F_{ex} \tag{5}$$

where:
M_d: virtual mass;
B_d: virtual damping coefficient;
K_d: virtual stiffness coefficient;
v_d: desired velocity;
F_{ex}: actual interaction force exerted on the robot handle.

Since the rehabilitation training robot operates under active motion control, it is unnecessary for the robot to exert a restoring force. As a result, the influence of the stiffness matrix can be disregarded. Consequently, as demonstrated in Ref. [31], the application of Euler discretization to Eq. (5) leads to the following discretized representation of the desired velocity:

$$v_d(n) = \frac{F_{ex}(n)\cdot\Delta t + M_d\cdot v_d(n-1)}{M_d + B_d\cdot\Delta t} \tag{6}$$

As shown in Eq. (6), the virtual mass M_d affects the response speed of the system. When M_d is large, the system exhibits stronger inertia and reduced compliance; when it is small, the system becomes more sensitive to external disturbances, which may lead to stability issues. The virtual damping coefficient B_d mainly influences the system's responsive compliance. A large damping coefficient reduces the system's ability to follow external forces, thereby affecting movement and decreasing the comfort of human-robot interaction. Conversely, if the damping coefficient is too small, although the system shows good adaptability, issues such as overshoot and instability may occur.

Therefore, in rehabilitation robot applications, it is significant to properly tune the virtual mass and damping parameters, so as to optimize the system's compliance and stability. To further improve the tracking performance and stability of the desired velocity generated by admittance control based on the measured interaction force, we introduce a compensation control method on the basis of an adaptive RBF neural network.

C. Tracking Error and Control Objective

Before constructing the inner-loop controller, it is imperative to define the tracking error and clarify its key role in the control system. This error serves as a bridge between the outer-loop admittance control and the inner-loop robust control, running throughout the entire control process. The admittance control module generates the desired velocity v_d based on the user's applied interaction force, reflecting the user's intended motion. In contrast, the actuator generates the actual velocity v, which signifies the robot's genuine dynamic response.

The discrepancy between the desired velocity and the actual velocity, defined as the velocity tracking error, is given in Eq. (7):

$$e_v = v_d - v \tag{7}$$

This error signal is simultaneously fed into the sliding mode controller and the RBF neural network disturbance estimator. It captures the deviation from the desired trajectory arising from modeling inaccuracies and external perturbations.

The inner-loop controller dynamically adjusts and compensates based on this error, enabling high-precision tracking of the desired velocity. In the proposed control strategy, the sliding mode component enhances robustness against disturbances and model uncertainties, while the neural network module estimates and compensates for unknown disturbances and modeling errors in real time through adaptive learning.

The primary objective of this study is to ensure that the system maintains a stable and precise response that closely aligns with the user's intended motion trajectory, even in the face of significant external disturbances or modeling deviations. The detailed architecture of the controller and the formulation of the control law will be elaborated on in the subsequent sections.

D. Sliding Mode Control and RBF Neural Network Estimation

1) Inner-loop robust control strategy

To ensure precise velocity tracking performance under exogenous disturbances and parametric uncertainties, this work develops a dual-layer inner-loop control architecture integrating nonlinear compensation techniques with an adaptive parameter estimation framework. The proposed controller, formulated based on the predefined velocity tracking error dynamics, establishes real-time compensation mechanisms for both model inaccuracies and external perturbations.

Although admittance control enables compliant human–robot interaction, it lacks the ability to actively compensate for system disturbances and parameter uncertainties. As a result, it often fails to ensure tracking accuracy under complex environmental conditions. To address this issue, a robust inner-loop control scheme is introduced as a supplement to the outer-loop admittance control.

The proposed inner-loop controller consists of two core modules: a sliding mode compensation term and a disturbance estimator based on an RBF neural network. The sliding mode component ensures exponential stability through discontinuous control action with boundary layer optimization, effectively suppressing high-frequency disturbances. Concurrently, the RBF-based observer implements gradient descent learning with Lyapunov-stable weight adaptation, enabling real-time compensation of unmodeled dynamics and nonlinear coupling effects through continuous approximation of lumped disturbances extracted from tracking error signals.

These two robust control methods together form a hybrid control strategy with strong disturbance rejection and high adaptability.

2) Sliding mode compensation term design

In motion control systems, tracking accuracy is often affected by parameter variations and system imperfections. To bolster the system's responsiveness across a spectrum of dynamic conditions, this research proposes the incorporation of a sliding mode compensation mechanism into the inner-loop controller, positioning it as a pivotal element of the robust control strategy.

This approach uses the velocity tracking error as the core input variable and constructs a nonlinear control term to achieve rapid error suppression. The compensation term is defined as shown in Eq. (8):

$$F_{smc} = k_s \, tanh(e_v) \tag{8}$$

where k_s is the control gain used to adjust the compensation strength, and $tanh(e_v)$ is a smooth nonlinear function that effectively reduces the high-frequency chattering typically caused by discontinuous control in traditional sliding mode methods. This adaptation not only enhances the smoothness of the control action but also increases its practical applicability.

The sliding mode compensation term plays a critical role in rapidly adjusting the system's dynamic response, especially in scenarios involving external perturbations, load variations, or actuator delays. This compensation module will be integrated with the neural network estimator in the final control law design.

3) Design of the RBF neural network disturbance estimator

To improve the control system's adaptability to unknown dynamic variations, an RBF neural network is incorporated into the inner-loop controller, functioning as a real-time disturbance estimator. This neural network employs the velocity tracking error as its input, facilitating online learning to effectively approximate the nonlinear uncertainties present within the system.

In a typical operational environment, the total disturbance impacting the system is multifaceted, encompassing external perturbations, frictional forces, and dynamics that may not be accurately modeled. Utilizing the universal approximation capabilities inherent in RBF networks, these unknown disturbances can be represented as shown in Eq. (9) [32]:

$$F_{total}(x, v) \approx F_{dist} + F_{fric} + \Delta(x, v) = W^{*T}\Phi(z) + \varepsilon \tag{9}$$

where W^* is the ideal weight vector of the neural network, and $\Phi(z)$ is the vector of Gaussian basis functions expressed as $\Phi(\mathrm{z}) = [\phi_1(z), \phi_2(z), \ldots, \phi_n(z)]^T$,where each basis function $\phi_{i(z)}$ is defined in Eq. (10):

$$\phi_{i(z)} = exp\left(\frac{(z-c_i)^2}{-2b_i{}^2}\right), \quad i = 1,2,\ldots,n. \tag{10}$$

where $z$denotes the input of the neural network, typically the velocity tracking error e_v; c_i represents the center of the i^{th} Gaussian basis function, determining the location of the basis function in the input space; b_i represents the width of the i^{th} Gaussian basis function, controlling the spread or influence range of each basis function; ε is the approximation error of the neural network, which satisfies $\varepsilon \le \varepsilon_{max}$, and ε is bounded.

To enable online adaptation, the weights of the RBF network are updated in real time using the adaptive law given in Eq. (11):

$$\dot{\hat{W}} = \gamma \Phi_{(z)} e_r \tag{11}$$

where $\gamma > 0$ is the learning rate, and the learning error e_r is defined as:

$$e_r = m(-\dot{e}_v - k_v e_v) - k_s \, tanh(e_v)$$

This adaptive update mechanism ensures that the network gradually converges to the actual disturbance characteristics, enabling the controller to compensate for dynamic uncertainties more effectively.

4) Control law formulation

In this section, we present the formulation of the final control law, which is derived from an analysis of the system dynamics and the previously established inner-loop modules. The control law is designed by synthesizing three key components: the desired dynamic behavior derived from the admittance controller, the nonlinear compensation term produced by the sliding mode controller, and the disturbance estimation provided by the RBF neural network.

The control input applied to the actuator is given by Eq. (12):

$$F_m = M(\dot{v}_d + k_v e_v) - F_{total}(x, v) + F_{smc} - F_{ex} \tag{12}$$

where F_m is the motor driving force; $\dot{v}_d$ represents the desired acceleration obtained from the admittance model; k_v is the velocity feedback gain; e_v is the velocity tracking error; F_{total} is the disturbance estimated by the RBF neural network; F_{smc} is the sliding mode compensation term; and F_{ex} is the external interaction force applied by the user.

This structure is designed to ensure a rapid response to user inputs, mitigate internal uncertainties, and compensate for unmodeled dynamics in real time. The inclusion of the nonlinear sliding mode term significantly enhances convergence during transient responses, while the adaptive neural network continually learns and adapts to varying conditions.

The resulting control law not only achieves precise velocity tracking but also upholds stability and robustness across a diverse range of operating scenarios. The effectiveness of the closed-loop implementation will be rigorously validated through simulation and experimental analyses in the subsequent sections.

5) Stability analysis based on the Lyapunov method

This analysis verifies whether the overall system, including both the nonlinear controller and adaptive estimator, ensures boundedness of tracking and estimation errors under uncertain conditions.

To verify the stability and convergence of the proposed RBF neural network compensation control strategy, the Lyapunov function is constructed for analysis.

First, the Lyapunov candidate function is defined in Eq. (13):

$$V = \frac{1}{2}Me_v^2 + \frac{1}{2}\widetilde{W}^T\gamma^{-1}\widetilde{W} \tag{13}$$

The weight estimation error of the neural network is defined as:

$$\widetilde{W} = W^* - \widehat{W}$$

where W^* is the ideal (optimal) weight vector and $\widehat{W}$ is the estimated weight vector updated during online learning.

This error term encapsulates the disparity between the estimated and optimal network parameters and serves a crucial role in evaluating convergence within the context of Lyapunov stability analysis. Within this function, the inaugural term signifies the kinetic energy associated with the tracking error, whereas the subsequent term denotes the energy related to the weight estimation error of the neural network.

Taking the time derivative of the above equation yields:

$$\dot{V} = Me_v\dot{e}_v + \widetilde{W}^T\gamma^{-1}\dot{\widetilde{W}}$$

According to the definition of the velocity tracking error, we have:

$$\dot{e}_v = \dot{v}_d - \dot{v}$$

From the control law:

$$F_m = M(\dot{v}_d + k_v e_v) - F_{total}(x, v) + k_s\, tanh(e_v) - F_{ex}$$

System dynamics:

$$M\dot{v} = F_m + F_{ex} - F_{dist} - F_{fric} - \Delta(x, v)$$

External disturbances approximated by the neural network [33]:

$$F_{total} = W^{*T}\Phi(z) + \varepsilon$$

By substituting the control law into the system dynamics, we obtain:

$$M(\dot{v}_d - \dot{v}) = -k_v Me_v - k_s tanh(e_v) + \widetilde{W}^T\Phi(z) + \varepsilon$$

That is,

$$M\dot{e}_v = -k_v Me_v - k_s\, tanh(e_v) + \widetilde{W}^T\Phi(z) + \varepsilon$$

Therefore,

$$Me_v\dot{e}_v = -k_v Me_v^2 - k_s e_v tanh(e_v) + e_v\left(\widetilde{W}^T\Phi(z) + \varepsilon\right)$$

Since$k_s > \varepsilon_{max}$, we have:

$$Me_v\dot{e}_v \le -k_v Me_v^2 - k_s\frac{e_v^2}{1 + |e_v|} + e_v\left(\widetilde{W}^T\Phi(z) + \varepsilon\right)$$

The adaptive weight update law is defined as:

$$\dot{\widehat{W}} = \gamma\Phi_{(Z)}e_r$$

where the neural network approximation error e_r is defined as:

$$e_r = m(\dot{v} - \ddot{x}_d - k_v e_v) - k_s\, tanh(e_v)$$

Consequently, we can conclude that:

$$\dot{\widetilde{W}} = \dot{W}$$

From these results, we derive:

$$\dot{\widetilde{W}} = -\dot{\widehat{W}} = -\gamma\Phi_{(z)}e_r:$$

Thus,

$$\widetilde{W}^T\gamma^{-1}\dot{\widetilde{W}} = -\widetilde{W}^T\Phi_{(z)}e_r$$

Upon substituting these expressions back, the derivative of the Lyapunov function can be expressed as:

$$\dot{V} \le -k_v Me_v^2 - k_s\frac{e_v^2}{1 + |e_v|} + \widetilde{W}^T\Phi_{(z)}e_r - \widetilde{W}^T\Phi_{(z)}e_r + e_v F_{total} + e_v\varepsilon$$

By eliminating the weight estimation error terms, the inequality can be simplified to:

$$\dot{V} \le -k_v Me_v^2 - k_s\frac{e_v^2}{1 + |e_v|} + e_v F_{total} + e_v\varepsilon$$

Assuming that F_{ex} remains bounded, and $k_s > \varepsilon_{max}$, an increase in k_s can ensure that e_v is ultimately bounded. This condition signifies that the system exhibits uniformly ultimate bounded stability. According to the principles of Lyapunov stability theory, by selecting appropriate control gains k_s and k_v, it is possible to maintain uniform asymptotic stability for the system. As a result, the tracking error e_v will eventually converge to a defined neighborhood of zero. Furthermore, the implementation of neural network-based compensation control proves effective in mitigating nonlinear disturbances, thereby enhancing the velocity tracking accuracy of the system.

E. Control Flow Diagram

To clearly illustrate the structure and signal interactions of the proposed control strategy, the control flow diagram is presented below. It reflects the real-time data processing and feedback mechanism implemented in the simulation experiments.

Fig. 3 illustrates the overall structure of the proposed control system for the rehabilitation robot. The system combines admittance control to generate compliant reference motion, sliding mode control to enhance robustness, and an RBF neural network for disturbance estimation and compensation, forming a closed-loop adaptive robust control architecture. The operational flow of the control strategy is as follows:

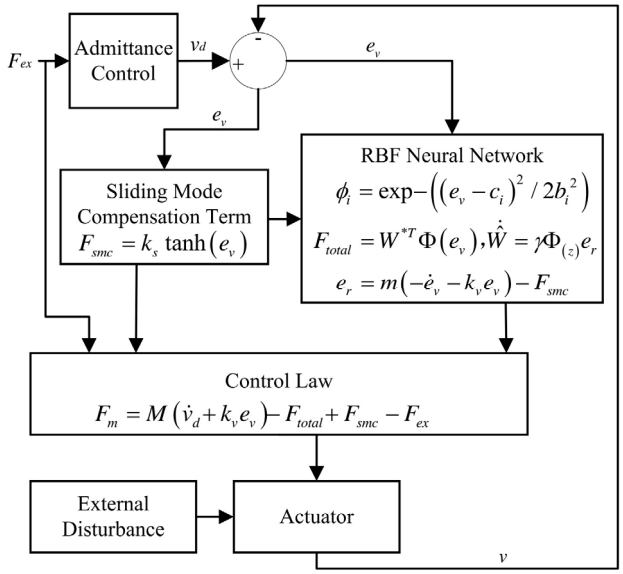

Fig. 3. Control flow diagram of the simulation.

Initially, the external force exerted by the user via the handle is transformed into a desired velocity command by the admittance control module, thereby encapsulating the user's intent for interaction. Subsequently, this desired velocity is juxtaposed with the actual actuator velocity to ascertain the tracking error.

Simultaneously, the error signal is processed through two pathways: it is directed to the sliding mode compensator and the RBF neural network module. The sliding mode controller devises a nonlinear compensation term derived from the tracking error, thereby enhancing the system's robustness in the face of modeling uncertainties and external disturbances. Concomitantly, the RBF neural network leverages the same error signal to estimate unknown disturbances and generate a corresponding compensation value. The network's weights undergo adaptive updates informed by the learning error, facilitating improved estimation accuracy over time.

The control law module amalgamates the desired dynamic response from the admittance controller, the compensation term supplied by the sliding mode controller, and the disturbance estimation from the RBF neural network. This integration yields the final control input, which is subsequently applied to the actuator.

As the actuator executes the prescribed motion, it remains susceptible to external disturbances. In real time, the actual velocity of the system is fed back to refresh the tracking error, thus establishing a robust closed-loop feedback control system.

The control framework that integrates admittance control, sliding mode compensation, and neural network estimation not only enables compliant human–robot interaction, but also effectively resists external disturbances and continuously optimizes control performance through adaptive learning, making it suitable for rehabilitation training tasks in complex environments.

IV. Result and Discussion

To thoroughly evaluate the efficacy of the proposed control method across a range of disturbances and operational requirements, a comprehensive series of simulations was conducted using the MATLAB platform. The analysis centered on three primary dimensions: (1) the resilience of the controller in the presence of external disturbances, (2) the influence of sliding mode gain on both control precision and operational smoothness, and (3) a comparative assessment against a conventional PID-based control strategy. Additionally, to substantiate the practical applicability of the proposed method, hardware-in-the-loop experiments were meticulously designed and executed.

To examine the robustness and adaptability of the controller, a simulation model that integrates admittance control, RBF neural network compensation, and sliding mode control was developed. This model aimed to evaluate the effectiveness of the proposed method in maintaining tracking performance amidst internal uncertainties and external disturbances.

A. MATLAB Simulation Setup

The simulation parameters are listed in Table I, encompassing the mechanical characteristics of the robot, the feedback control gains, and the structure of the RBF network. In the course of the simulation, an interaction force mimicking voluntary input from the patient was applied to the human-robot system. Additionally, a complex external disturbance was introduced to evaluate the system's capacity for disturbance rejection.

TABLE I. Parameters of the Simulation Control System

Parameter	Symbol	Value
Virtual Mass	m_d	0.5 kg
Actual Mass	m	0.5 kg
Virtual Damping	b_d	6 Ns/m
Velocity Feedback Gain	k_v	120
Sliding Mode Control Gain	k_s	10
RBF Learning Rate	γ	2
Number of Neurons	N	30
Basis Function Centers	c	[−3, 3]
Basis Function Width	b	1.5

The interaction force was defined as a sinusoidal signal:

$$F_{ex} = 10\,sin\left(2t_{(i)}\right)$$

The external disturbance was modeled as:

$$F_{total} = -20sin\left(2t_{(i)}\right) - 10cos\left(1.5t_{(i)}\right)$$

These inputs were designed to simulate realistic dynamic loads encountered in rehabilitation scenarios. The simulation results, including position tracking, velocity tracking, and control force, were employed to assess the controller's tracking accuracy, dynamic stability, and robustness.

The MATLAB simulation was conducted based on the aforementioned configuration, and the resulting performance profiles are presented in Fig. 4. It is important to highlight that, in the absence of the RBF neural network control method, a conventional admittance combined with sliding mode control strategy is employed, where the control law is defined as follows:

$$F_m = M(\dot{v}_d + k_v e_v) + F_{smc} - F_{ex}$$

All parameters remain consistent with those used in the RBF neural network control method.

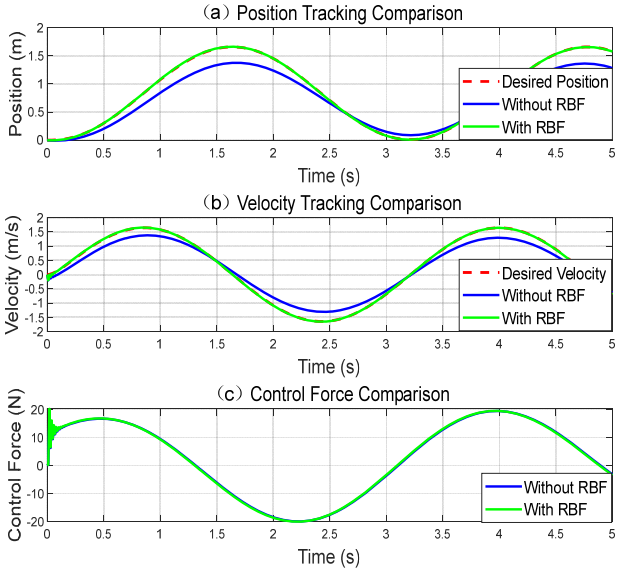

Fig. 4. MATLAB simulation results.

Fig. 4 presents the simulation results of the system under external disturbances, highlighting a comparison of performance between scenarios with and without RBF neural network compensation. The analysis focuses on three critical aspects: position tracking, velocity tracking, and control force response. Notably, the incorporation of the RBF network substantially enhances tracking accuracy, response speed, and robustness in the face of disturbances.

In Fig. 4(a), the actual position deviates considerably from the desired trajectory when the RBF module is not used, especially near turning points where dynamic changes occur. When RBF compensation is utilized, the system displays markedly improved path-following capabilities, with reduced steady-state and transient errors. These advancements indicate that the RBF neural network effectively addresses modeling uncertainties and adapts to time-varying disturbances, thereby significantly enhancing motion control precision in complex environments.

Fig. 4(b) highlights the velocity tracking results. In the scenario without RBF support, a pronounced phase lag and larger error margins are observed, especially during high-acceleration phases. In contrast, the RBF-based controller demonstrates a close alignment with the reference velocity profile, underscoring its ability to compensate for nonlinearity, friction, and time-varying dynamics, the proposed strategy produces smoother velocity transitions and suppresses fluctuations typically encountered with conventional methods.

Fig. 4(c) compares the motor force outputs. In both cases, the control inputs remain smooth and continuous. However, the RBF-enhanced method exhibits slightly reduced peak force amplitudes, which implies improved energy efficiency and better compliance during interaction.

B. Accuracy of Disturbance Estimation by RBF Neural Network

In addition to tracking performance, the ability of the RBF neural network to reliably identify external disturbances in real time is critical to achieving robust control. This estimation mechanism underpins the controller's capacity to reject uncertainties and adapt to varying environments. As shown in Fig. 5, the actual applied disturbance is compared against the signal inferred by the neural network, providing a clear view of the estimator's responsiveness and precision.

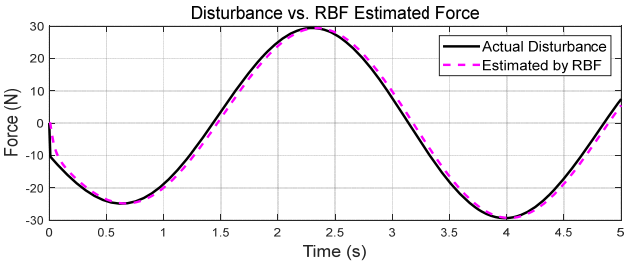

Fig. 5. Comparison between the actual external disturbance and the output estimated by the RBF neural network.

The figure reveals that the predicted disturbance trajectory aligns closely with the true signal in terms of both amplitude and phase—particularly during periods of rapid change or peak deviation. This close correspondence indicates that the network effectively learns the dynamic behavior of the disturbance through continuous online adaptation.

Even in the presence of sharp fluctuations, the RBF observer maintains a high level of accuracy. Such real-time adaptability allows the control system to respond proactively, mitigating the influence of unknown forces before they degrade performance. By integrating this adaptive capability within the feedback loop, the overall system gains enhanced resilience against nonlinearities, frictional forces, and unmodeled dynamics.

Ultimately, the estimation prowess of the RBF neural network is the cornerstone of the improvements illustrated in Fig. 4. In the absence of the neural network's contributions, the controller would have been relegated to relying solely on fixed structural terms, which frequently

prove inadequate in the face of dynamic or unpredictable operating conditions.

C. Comparative Evaluation between PID-Based and RBF-Based Disturbance Compensation

To assess the efficacy of the proposed disturbance compensation strategy utilizing the RBF neural network, a comparative simulation study was conducted within an identical dual-loop control framework. The baseline methodology employs a conventional PID controller for disturbance estimation, while the proposed approach replaces it with an adaptive RBF neural network. Both strategies incorporate an admittance-based outer loop responsible for generating reference trajectories and a sliding mode controller in the inner loop for velocity tracking. The primary distinction between the two approaches lies in the configuration of the disturbance compensation term.

In the PID-based scheme, the compensation force is constructed using a proportional–integral–derivative controller. The total control input F_m applied to the system is given by:

$$F_m = m(\dot{v}_d + k_v e_v) + F_{PID} + F_{smc} - F_{ex}$$

$$F_{PID} = K_p e_v + K_i \int_0^t e_v(t)dt + K_d \dot{e}_v$$

The parameters of the PID controller were set to $K_p = 4$, $K_i = 5$, and $K_d = 0.05$. Although this configuration permits straightforward implementation, it is insufficiently adaptable to effectively manage time-varying or nonlinear disturbances. The results of the simulations comparing the two control strategies are presented in Fig. 6.

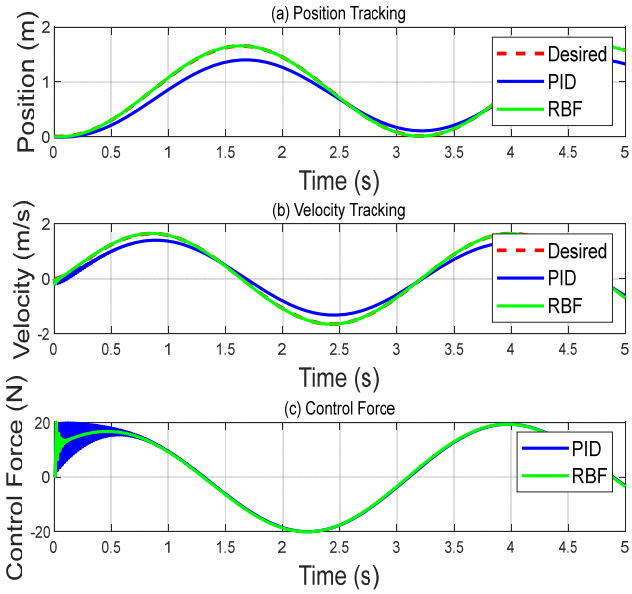

Fig. 6. Comparison of velocity tracking and control force responses under PID and RBF compensation.

To facilitate a quantitative comparison between the two methodologies, we analyzed three key performance indicators: RMSE, maximum tracking error, and recovery time. In this context, recovery time is defined as the shortest duration during which the velocity tracking error remains continuously within ±0.1 m/s for a minimum of 0.3 s.

The results are summarized in Table II. The proposed RBF-based strategy outperformed the PID-based method across all metrics. Specifically, RMSE was reduced from 0.2192 m/s to 0.0133 m/s, indicating a 93.9% improvement. The maximum velocity error decreased from 0.3305 m/s to 0.2012 m/s, a reduction of 39.1%. Most significantly, the recovery time dropped from 1.27 s to 0.04 s, corresponding to a 96.9% improvement in dynamic response.

TABLE II. QUANTITATIVE COMPARISON BETWEEN PID-BASED AND RBF-BASED DISTURBANCE COMPENSATION STRATEGIES

Metric	PID-Based	RBF-Based	Improvement (%)
RMSE (m/s)	0.2192	0.0133	93.9
Max Error (m/s)	0.3305	0.2012	39.1
Recovery Time (s)	1.27	0.04	96.9

These findings demonstrate that the adaptive learning capability of the RBF neural network enables more accurate disturbance estimation, allowing the system to respond quickly and robustly under varying external conditions. In contrast, the PID-based method exhibits limited adaptability and slower convergence when facing complex dynamic disturbances.

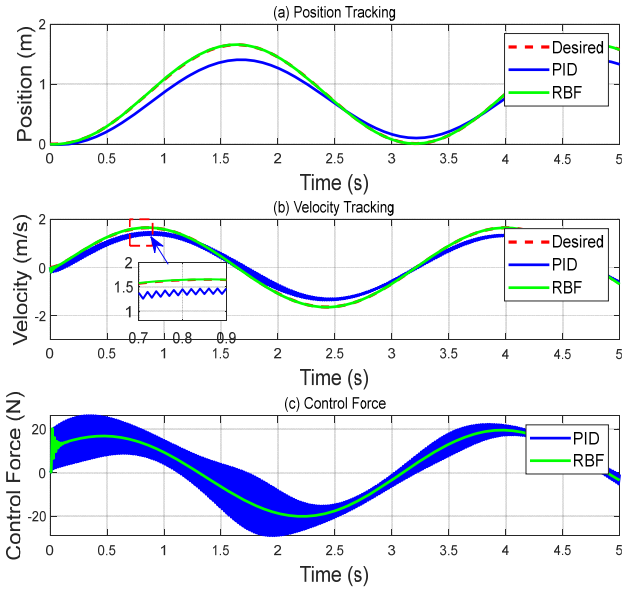

Fig. 7. PID control improves tracking accuracy but induces oscillations.

Furthermore, within the control framework incorporating admittance control, sliding mode regulation, and PID-based disturbance compensation, considerable velocity chattering was observed upon a moderate increase in PID parameters. As shown in Fig. 7, with the parameter settings of $K_p = 6$, $K_i = 5$, and $K_d = 0.05$, the system exhibited significant oscillations in the velocity response during dynamic transitions, which adversely affected the overall control stability. This result indicates that although PID compensation is easy to implement, it has limited

adaptability when facing complex external disturbances and nonlinear dynamics. In contrast, the compensation strategy based on RBF neural networks demonstrated superior robustness and stability under the same conditions.

D. Performance Comparison under Various Disturbance Conditions

To rigorously assess the robustness and adaptive capabilities of the proposed control strategy, we conducted simulation experiments across three distinct disturbance scenarios: reduced disturbance, normal disturbance, and increased disturbance. Each scenario involved a comparison between two approaches: the traditional admittance and sliding mode control method (Without RBF) and the proposed approach (With RBF), which integrates an adaptive RBF neural network.

1) Reduced disturbance

In the first scenario, the external disturbance was set to a lower magnitude, expressed as follows:

$$F_{total} = -5\,sin(2t_{(i)}) - 2\,cos(1.5t_{(i)})$$

The simulation results are shown in Fig. 8.

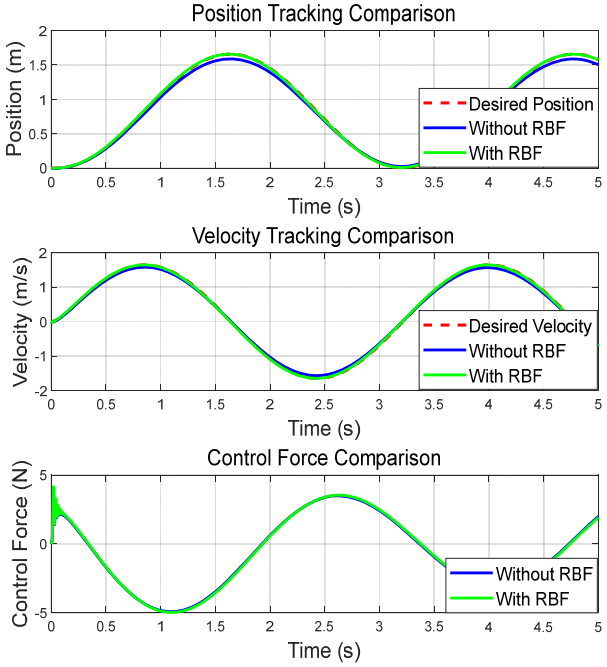

Fig. 8. MATLAB simulation results under reduced external disturbance.

Under mild disturbance conditions, both methodologies exhibited commendable performance in accurately tracking the desired trajectories. However, the RBF-enhanced method demonstrated superior accuracy, with significantly reduced tracking errors and smoother force outputs. The improvement was particularly clear in response stability and recovery speed.

2) Normal disturbance

For this scenario, a moderate external disturbance was introduced, given by:

$$F_{total} = -20sin(2t_{(i)}) - 10cos(1.5t_{(i)})$$

The simulation results presented earlier in Fig. 4 unequivocally illustrate the distinct advantages of the RBF-based approach. Notably, there was a marked enhancement in trajectory accuracy, complemented by smoother velocity profiles and diminished fluctuations in control forces. These findings underscore the efficacy of the proposed neural network-enhanced controller in adeptly counteracting moderate disturbances commonly encountered in practical scenarios.

3) Increased disturbance

To challenge the system's robustness further, the external disturbance was substantially increased, as defined by:

$$F_{total} = -50\,sin(2t_{(i)}) - 20\,cos(1.5t_{(i)})$$

The simulation results are shown in Fig. 9.

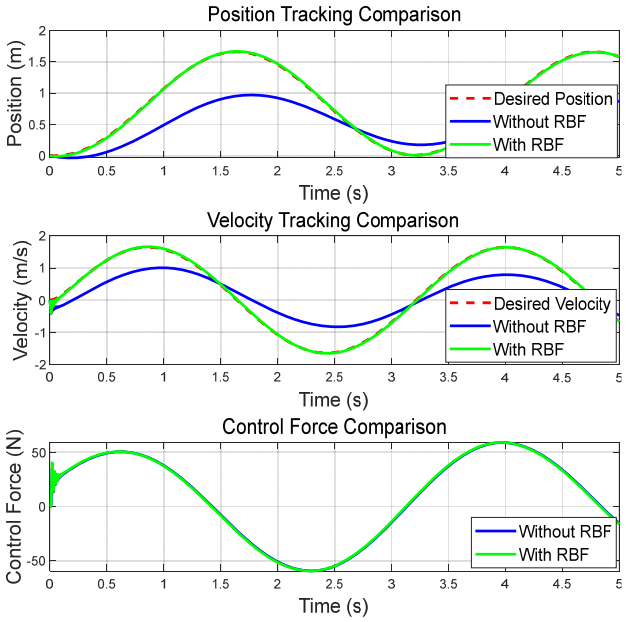

Fig. 9. MATLAB simulation results for increasing external perturbation.

In this severe disturbance scenario, the performance of the conventional method without RBF deteriorated sharply, exhibiting significant deviations from the desired trajectory, pronounced oscillations, and delayed recovery times. Conversely, the approach that incorporated RBF compensation demonstrated markedly superior accuracy and exhibited enhanced resilience and adaptability. Such outcomes underscore the tangible advantages of integrating RBF neural networks into the control framework when confronted with challenging conditions.

To provide a comprehensive assessment of robustness and adaptability, three key indices were extracted from each simulation run:

RMSE—root-mean-square velocity error;

Max Error—the peak magnitude of the velocity error;

Recovery Time—the first instant at which the absolute velocity error $|e_v|$ remains inside ±0.05 m/s for a *continuous* 0.50 s window.

Three disturbance levels were tested: reduced, normal and increased. For each disturbance level, we conducted a comparative analysis between the "without-RBF" admittance combined with a sliding-mode controller and the proposed RBF-assisted controller. The numerical findings are compiled in Table III, where the percentages highlighted in blue denote the relative enhancements achieved through the integration of the RBF neural-network compensator.

Quantitative results for each scenario are summarized in Table III, providing a clear comparison between the two approaches:

TABLE III. TRACKING PERFORMANCE UNDER DIFFERENT DISTURBANCE CONDITIONS

Disturbance Level	Method	RMSE (m/s)	Improvement (%)	Max Error (m/s)	Improvement (%)	Recovery Time (s)	Improvement (%)
Reduced	Without RBF	0.0548	66.4%	0.0864	59.3%	<0.01	0.0%
	With RBF	0.0195		0.0352		<0.01	
Normal	Without RBF	0.2319	94.3%	0.3503	42.6%	n/a[1]	-
	With RBF	0.0133		0.2012		0.06	
Increased	Without RBF	0.5658	95.0%	0.8552	51.7%	n/a[1]	-
	With RBF	0.0285		0.4132		0.08	

Note: The ±0.05 m s^{-1} for 0.50 s rule mirrors the tolerance band used in our laboratory trials. If this band is never held for the required duration within the 5 s simulation window, the recovery time is reported as n/a.

The presented figures illustrate a distinct trend: as the level of disturbance increases, the performance disparity between the two control strategies becomes increasingly evident. At the highest disturbance level, the conventional controller (devoid of RBF integration) exhibits an RMSE of 0.5658 m/s and a maximum velocity error of 0.8552 m/s. This controller does not achieve recovery within the specified ±0.05 m/s tolerance for 0.5 s, resulting in a "n/a" recovery time as indicated in Table III. In contrast, the proposed RBF-enhanced strategy markedly enhances performance, achieving an RMSE of 0.0285 m/s—representing a 95.0% decrease—and a maximum error of 0.4132 m/s, with a successful recovery time of 0.08 s. Even under conditions of minimal disturbances, the RMSE notably decreases from 0.2319 m/s to 0.0133 m/s (a substantial improvement of 94.3%), while the recovery time is reduced from "n/a" to 0.06 s. Such consistent advancements in tracking accuracy, disturbance rejection, and dynamic recovery accentuate the practicality of integrating an adaptive RBF module into the control architecture of rehabilitation robots, particularly in unpredictable or dynamically fluctuating environments.

Moreover, these consistent enhancements in tracking precision, control stability, and responsiveness affirm the practical efficacy of incorporating neural network-based compensation into the control strategies of rehabilitation robots. This methodology proves especially advantageous in real-world scenarios characterized by unpredictable or variable disturbances.

Consequently, in situations where external disturbances are minimal and computational resources for the control system are constrained, pure sliding mode control may be adequate. However, since RBF-based control necessitates greater memory and processing capabilities, it is particularly suited for applications that demand high precision or rapid dynamic responses. It is noteworthy that in this study, supplementary integral terms with appropriate gains $k_v e_v$ were introduced to mitigate velocity tracking errors. This suggests that relying on a single control method to correct velocity errors often fails to achieve ideal results in practice.

E. Experimental Validation in the Laboratory

To ascertain the practical effectiveness of the proposed control strategy, a series of experimental tests were conducted utilizing a physical prototype platform developed in the laboratory. As depicted in Fig. 10, the system consists of two orthogonally arranged linear motion modules that together form a planar X–Y motion platform. Each module is actuated by a ball screw mechanism powered by a 200 W DC servo motor (manufactured by Kinco, Shenzhen, China), and is supplemented by a rotary encoder for precise velocity feedback. Additionally, a two-dimensional force sensor, with a measuring range of ±200 N in both X and Y directions and a resolution of ±1 N, is positioned below the handle to continuously monitor the interaction forces applied by the user. The control algorithm operates on a dSPACE DS1104 real-time control unit, maintaining a control loop frequency of 1 kHz.

Throughout the experimental trials, participants were allowed to apply force freely to the handle, while the controller employed an admittance control approach to convert this force into a desired velocity. Under the proposed robust control strategy enhanced by RBF neural network compensation, the system responded smoothly. Distinct from conventional trajectory tracking tasks, this particular experiment eschewed predefined motion paths, instead simulating a rehabilitation training scenario wherein users actively manipulated the handle. The primary focus was to evaluate the compliance and responsiveness of the human–robot interaction without relying on preset trajectories.

Each training session varied in duration from 5 to 20 min, contingent upon the participant's physical condition and fatigue levels. Notably, throughout the entire session, no transitions to different control modes were made—the system remained in active control mode, dynamically adjusting its response in real-time to the interaction forces exerted by the user.

As illustrated in Fig. 11, the velocity of the handle exhibited a close correlation with the variation trends of the interaction force, signifying exceptional compliance and responsiveness. Even in the face of abrupt changes or intentional perturbations, the system maintained stable operation, exhibiting no significant overshoot, delay, or oscillation. These findings underscore the robust adaptability and disturbance rejection capabilities of the proposed control framework under dynamic conditions.

Overall, the experimental results confirm the feasibility of the proposed "admittance control + RBF neural network compensation + sliding mode robust control" strategy for real-world rehabilitation robots. This approach enables natural and real-time human–robot interaction, delivers smooth and safe motion, and holds significant potential for practical deployment in clinical or home-based rehabilitation training systems.

Fig. 10. Prototype experimental verification.

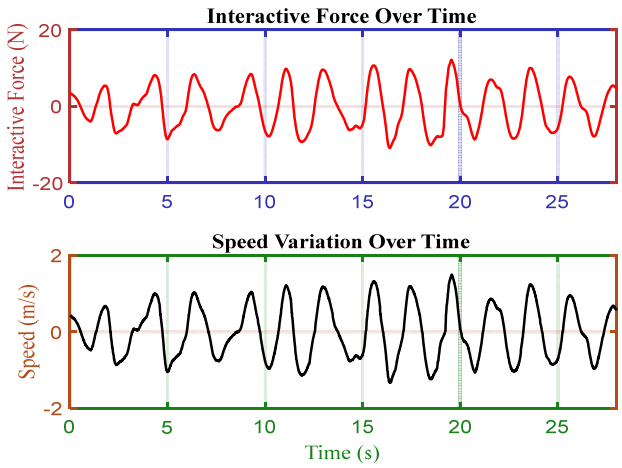

Fig. 11. Curves of collected interaction force and corresponding velocity variation.

V. Conclusion

This paper proposes a two-dimensional rehabilitation robot control strategy based on admittance control and adaptive RBF neural network compensation, primarily targeting upper-limb rehabilitation for patients with residual muscle strength and voluntary motor capabilities.

In practical motion control, constructing precise mathematical models for friction and external disturbances is challenging. Moreover, modeling errors in the derived dynamic equations are inevitable. When using only admittance control and sliding mode control to achieve compliant interaction, the system performs well under small disturbances; however, as unmodeled uncertainties and external disturbances increase, the tracking performance significantly degrades, thereby compromising control compliance and patient comfort.

To address these challenges, an RBF neural network was integrated into the control framework. This controller enables real-time estimation and compensation of external disturbances and friction, effectively improving the system's compliance under disturbed conditions. Additionally, it adapts to sudden changes in interaction force, ensuring smooth and compliant motion during handle manipulation.

Nonetheless, some limitations remain in the current study. The experiments were conducted exclusively in a laboratory setting with healthy participants, and the interaction mode was simplified. Clinical validation involving real patients with complex neuromuscular impairments has not been conducted. Furthermore, although the RBF-based compensation enhances adaptability, it imposes relatively high computational demands, which may create performance bottlenecks during long-term use or when deploying the system on low-cost embedded devices.

Therefore, future work will involve collaboration with rehabilitation medical institutions to conduct formal clinical trials, assessing the system's effectiveness, comfort, and safety in real rehabilitation scenarios, as well as analyzing its long-term impact on patient outcomes. Additionally, efforts will be directed toward the optimization of the control algorithm to facilitate efficient operation on lightweight embedded platforms, with the objective of achieving an optimal balance between real-time responsiveness and control performance.

Conflict of Interest

The authors declare no conflict of interest.

Author Contributions

Conceptualization, IVM and TBD; methodology, IVM; software, GW; validation, GW and IVM; formal analysis, GW and ZZD; investigation, IVM and TBD; resources, IVM and TBD; data curation, GW and ZZD; writing—original draft preparation, GW and ZZD; writing—review and editing, IVM and TBD; visualization, GW; supervision, IVM; all authors had approved the final version.

References

[1] A. Garcia-Gonzalez, R. Q. Fuentes-Aguilar, I. Salgado *et al.*, "A review on the application of autonomous and intelligent robotic

devices in medical rehabilitation," *J. Braz. Soc. Mech. Sci. Eng.*, vol. 44, 393, 2022.
[2] F. Yakub, A. Z. M. Khudzari, and Y. Mori, "Recent trends for practical rehabilitation robotics, current challenges and the future," *Int. J. Rehabil. Res.*, vol. 37, no.1, pp. 9–21, 2014.
[3] M. Osman, N. Azlan, I. Suwarno *et al.,* "Self-motion control exoskeleton for upper limb rehabilitation with perceptron neuron motion capture," *Int. J. Robot. Control Syst.*, vol. 5, no. 1, pp. 500–515, 2025.
[4] S. Qiu, Z. Pei, C. Wang *et al.,* "Systematic review on wearable lower extremity robotic exoskeletons for assisted locomotion," *J. Bionic Eng.,* vol. 20, pp. 436–469, 2023.
[5] L. Xuan, Y. Shen, X. Yang *et al.,* "A review of the development status of exoskeleton robots for lower extremity rehabilitation," in *Proc. 2022 Int. Symp. Control Eng. Robot. (ISCER)*, Beijing, 2022, pp. 20–25.
[6] A. A. Moshaii, M. M. Moghaddam, and V. D. Niestanak, "Fuzzy sliding mode control of a wearable rehabilitation robot for wrist and finger," *Ind. Robot.*, vol. 46, pp. 839–850, 2019.
[7] M. Schwenzer, M. Ay, T. Bergs *et al.,* "Review on model predictive control: An engineering perspective," *Int. J. Adv. Manuf. Technol.*, vol. 117, pp. 1327–1349, 2021.
[8] K. Nizamis, A. Athanasiou, S. Almpani *et al.,* "Converging robotic technologies in targeted neural rehabilitation: A review of emerging solutions and challenges," *Sensors*, vol. 21, no. 6, 2084, 2021.
[9] D. Xu, D. Zhao, J. Yi *et al.,* "Trajectory tracking control of omnidirectional wheeled mobile manipulators: Robust neural network-based sliding mode approach," *IEEE Trans. Syst. Man Cybern. B Cybern*., vol. 39, pp. 788–799, 2009.
[10] H. Shraim, A. Awada, and R. Youness, "A survey on quadrotors: Configurations, modeling and identification, control, collision avoidance, fault diagnosis and tolerant control," *IEEE Aerosp. Electron. Syst. Mag.*, vol. 33, pp. 14–33, 2018.
[11] J. Cao, S. Q. Xie, R. Das *et al.,* "Control strategies for effective robot assisted gait rehabilitation: The state of art and future prospects," *Med. Eng. Phys.*, vol. 36, pp. 1555–1566, 2014.
[12] L. Ding, H. Xing, A. Torabi *et al*., "Intelligent assistance for older adults via an admittance-controlled wheeled mobile manipulator with task-dependent end-effectors," *Mechatronics*, vol. 85, 102821, 2022.
[13] M. Lin, H. Wang, J. Niu *et al.,* "Adaptive admittance control scheme with virtual reality interaction for robot-assisted lower limb strength training," *Machines*, vol. 9, no. 11, 301, 2021.
[14] J. Hu, H. Zhang, H. Liu *et al.,* "A survey on sliding mode control for networked control systems," *Int. J. Syst. Sci.*, vol. 52, pp. 1129–1147, 2021.
[15] J. Shi, L. Xu, G. Cheng *et al.,* "Trajectory tracking control based on RBF neural network of the lower limb rehabilitation robot," *Proc. IEEE Int. Conf. Mechatronics Autom.,* pp. 117–123, 2020.
[16] Q. Liu and Q. Cong, "Kinematic and dynamic control model of wheeled mobile robot under internet of things and neural network," *J. Supercomput.*, vol. 78, pp. 8678–8707, 2022.
[17] U. Riaz, M. Tayyeb, and A. A. Amin, "A review of sliding mode control with the perspective of utilization in fault tolerant control," *Recent Adv. Electr. Electron. Eng.*, vol. 14, no. 3, pp. 312–324, 2021.
[18] H. H. M. Al-Almoodi, N. Z. Azlan, I. Shahdad *et al.,* "Continuous passive motion machine for elbow rehabilitation," *Int. J. Robot. Control Syst.*, vol. 1, no. 3, pp. 402–415, 2021.
[19] I. Zaway, R. Jallouli-Khlif, B. Maaleja *et al.,* "Multi-objective fractional order PID controller optimization for kid's rehabilitation exoskeleton," *Int. J. Robot. Control Syst.*, vol. 3, no. 1, pp. 32–49, 2022.
[20] S. Mihai, M. Yaqoob, D. V. Hung *et al.*, "Digital twins: A survey on enabling technologies, challenges, trends and future prospects," *IEEE Commun. Surv. Tutor.*, vol. 24, no. 4, pp. 2255–2291, 2022.
[21] A. Plaat, W. Kosters, and M. Preuss, "High-accuracy model-based reinforcement learning, a survey," *Artif. Intell. Rev.*, vol. 56, no. 9, pp. 9541–9573, 2023.
[22] S. M. Amrr and A. Alturki, "Robust control design for an active magnetic bearing system using advanced adaptive SMC technique," *IEEE Access*, vol. 9, pp. 155662–155672, 2021.
[23] D. A. Dever, N. A. Sonnenfeld, M. D. Wiedbusch *et al.*, "A complex systems approach to analyzing pedagogical agents' scaffolding of self-regulated learning within an intelligent tutoring system," *Metacognition Learn.*, vol. 18, no. 3, pp. 659–691, 2023.
[24] Z. Adeola-Bello and N. Azlan, "Power assist rehabilitation robot and motion intention estimation," *Int. J. Robot. Control Syst.*, vol. 2, no. 2, pp. 297–316, 2022.
[25] D. F. Brown and S. Q. Xie, "Effectiveness of intelligent control strategies in robot-assisted rehabilitation—A systematic review," *IEEE Trans. Neural Syst. Rehabil. Eng.*, vol. 32, pp. 1828–1840, 2024.
[26] S. C. Yogi, V. K. Tripathi, and L. Behera, "Adaptive integral sliding mode control using fully connected recurrent neural network for position and attitude control of quadrotor," *IEEE Trans. Neural Netw. Learn. Syst*., vol. 32, no. 12, pp. 5595–5609, 2021.
[27] W. Qian, J. Liao, L. Lu *et al.,* "CURER: A lightweight cable-driven compliant upper limb rehabilitation exoskeleton robot," *IEEE/ASME Trans. Mechatron.*, vol. 28, pp. 1730–1741, 2022.
[28] D. Wu, X. T. Ha, Y. Zhang *et al.,* "Deep-learning-based compliant motion control of a pneumatically-driven robotic catheter," *IEEE Robot. Autom. Lett.*, vol. 7, pp. 8853–8860, 2022.
[29] C. Yang, G. Peng, L. Cheng *et al.,* "Force sensorless admittance control for teleoperation of uncertain robot manipulator using neural networks," *IEEE Trans. Syst. Man Cybern. Syst.*, vol. 51, pp. 3282–3292, 2019.
[30] M. Grotjahn, M. Daemi, and B. Heimann, "Friction and rigid body identification of robot dynamics," *Int. J. Solids Struct.*, vol. 38, no. 10–13, pp. 1889–1902, 2001.
[31] Y. Han, J. Wu, C. Liu *et al.,* "An iterative approach for accurate dynamic model identification of industrial robots," *IEEE Trans. Robot.*, vol. 36, pp. 1577–1594, 2020.
[32] H. Wang, X. Zhou, and Y. Tian, "Robust adaptive fault-tolerant control using RBF-based neural network for a rigid-flexible robotic system with unknown control direction," *Int. J. Robust Nonlinear Control*, vol. 32, no. 3, pp. 1272–1302, 2022.
[33] H. Yang and J. Liu, "An adaptive RBF neural network control method for a class of nonlinear systems," *IEEE/CAA J. Autom. Sin.*, vol. 5, pp. 457–462, 2018.